1

DESIGN AND DEVELOPMENT OF A COMPOSITE DOME FOR EXPERIMENTAL CHARACTERIZATION OF MATERIAL PERMEABILITY

Hector Estrada, Assistant Professor
Department of Civil and Environmental Engineering
Vanderbilt University
Box 44, Station B
Nashville, TN 37235
Ph: (615) 343–4562, e–mail: estrada@vuse.vanderbilt.edu

Stanley S. Smeltzer, III, Research Engineer
MS 190, Structural Mechanics Branch
NASA Langley Research Center
Hampton, VA 23681–2199

ABSTRACT

This paper presents the design and development of a carbon fiber reinforced plastic dome, including a description of the dome fabrication, method for sealing penetrations in the dome, and a summary of the planned test series. This dome will be used for the experimental permeability characterization and leakage validation of composite vessels pressurized using liquid hydrogen and liquid nitrogen at the Cryostat Test Facility at the NASA Marshall Space Flight Center (MSFC). The preliminary design of the dome was completed using membrane shell analysis. Due to the configuration of the test setup, the dome will experience some flexural stresses and stress concentrations in addition to membrane stresses. Also, a potential buckling condition exists for the dome due to external pressure during the leak testing of the cryostat facility lines. Thus, a finite element analysis was conducted to assess the overall strength and stability of the dome for each required test condition. Based on these results, additional plies of composite reinforcement material were applied to local regions on the dome to alleviate stress concentrations and limit deflections. The dome design includes a circular opening in the center for the installation of a polar boss, which introduces a geometric discontinuity that causes high stresses in the region near the hole. To attenuate these high stresses, a reinforcement system was designed using analytical and finite element analyses. The development of a low leakage polar boss system is also investigated.

INTRODUCTION

Cryogenic fluids have been used successfully for space propulsion systems since the 1950s. In fact, they are the main fuel components of most propulsion systems in the United States today. The traditional containment vessel for these cryogenic fluids has exclusively been metallic. However, because of the need to reduce the overall weight of space vehicles, composite materials are now being considered as a possible alternative to metallic materials. In the pressure vessel industry, composites have successfully contained low-pressure fluids and gases. A concern associated with storing cryogenic fluids in a composite pressure vessel is the diffusion of the fluid through the tank wall, since composites are more porous than metals. Typically, this material permeability problem has been addressed by using metallic liners, since limited information on composite material permeability at cryogenic conditions exists. Although lined composite pressure vessels offer significant weight savings over their metallic counterparts, the liner adds unnecessary weight and reduces potential payload. Therefore, a program was initiated to investigate the material permeability characteristics and methods for sealing penetrations for liner-less composite vessels containing pressurized cryogenic liquids.

This paper describes the design and development of a carbon fiber reinforced plastic (CFRP) pressure vessel to be used as a test article in the experimental permeability characterization of composite materials. The composite dome test article will be subjected to thermal and pressure cyclic loading using liquid hydrogen and liquid nitrogen. A complete summary of the research project is given with a focus on the design of the structural system and the development of the access system. The paper is organized as follows. First, we describe the dome and the cryostat setup. Then, we describe the failure modes for the dome. We cover the analysis and design process next, followed by a brief description of the dome polar boss sealing system.

DESCRIPTION OF THE DOME AND CRYOSTAT SETUP

The test article is a one-piece carbon/epoxy composite hemispherical dome cap and flange. The dome cap has an eighty-inch (2,032 mm – millimeters) radius and an axial height, *H*, of approximately six inches (152 mm). The flange extends five inches (127 mm) outward from the outside edge of the dome cap and is oriented perpendicular to the dome center line shown in the dome cross-section in Fig. 1. A cross-sectional view of the test article is given in Fig.1. Figure 2 depicts an exploded view of the Cryostat Test Facility (CTF) assembly containing the test article. The test article's geometry and dimensions were chosen to accommodate the existing CTF, as shown in Fig. 2, as well as simulate geometric scale of Reusable Launch Vehicle (RLV) hardware. The test article was fabricated with Hercules IM7/8552 preimpregnated (or prepreg) carbon/epoxy, plain weave fabric using the hand lay-up fabrication method. A single piece aluminium tool was used for both fabrication and curing of the test article. Forty-five degree gore sections of fabric that began at the center of the dome and extended to the outside edge of the flange

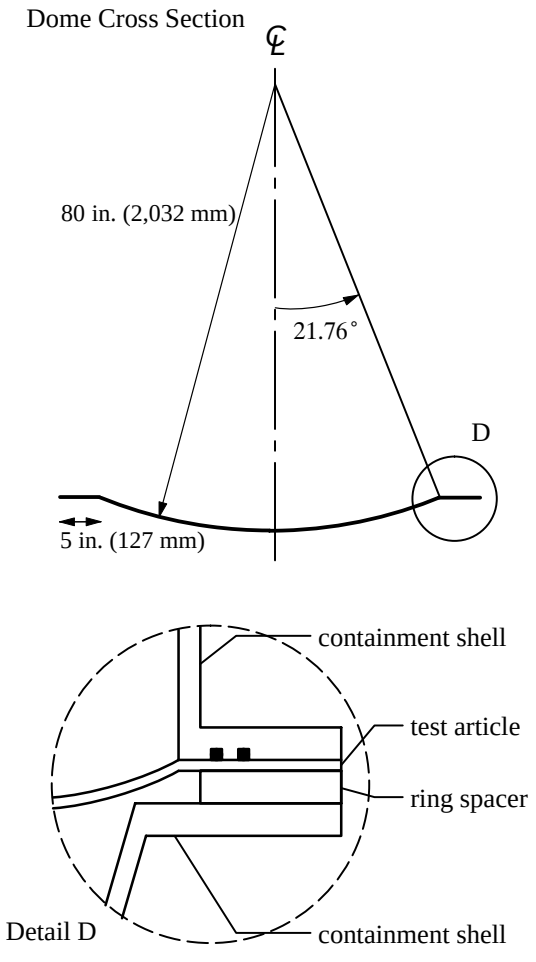

Figure 1: Geometry of Intact Dome.

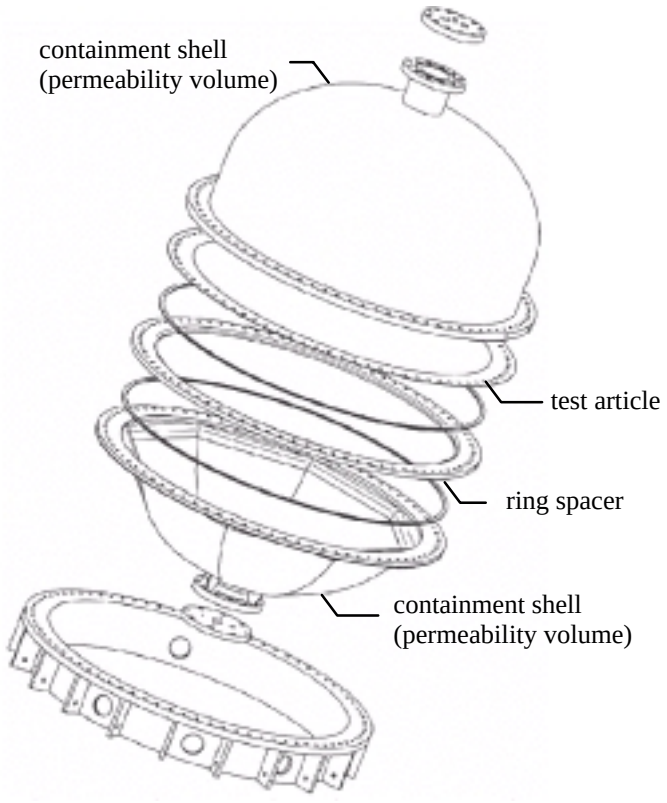

Figure 2: Cryostat Assembly.

were cut and aligned on the tool. Subsequent plies were "clocked" at fifteen-degree increments around the tool to keep from aligning cuts through the thickness of the laminate. The laminate configuration for the test article is $[0°/90°, \pm 45°]_{3S}$, which produced a twelve ply, 0.12 inch (3 mm) nominal thickness, quasi-isotropic laminate for the entire dome cap. The next fabrication step for the test article involved placing reinforcing plies along the flange to dome interface. Details of this reinforcement design will be described in the analysis section. A typical 350 °F (176.7 °C) curing cycle was employed to cure the test article. The final step in the fabrication of the test article involved drilling a hole pattern along the circumference of the flange. This hole pattern matches that of the upper and lower domes (containment shells) of the CTF, which are bolted together to perform the testing. The intact test article will be used to perform the first phase of the testing for material permeability. After the first phase of testing is complete, the dome will be modified to include an access hole in the center of the dome, which is meant to simulate a typical tank sump or vent opening. A polar boss sealing system, shown in Fig. 3 and described in a later section, will be used to seal the access hole in preparation of the second phase of the test series.

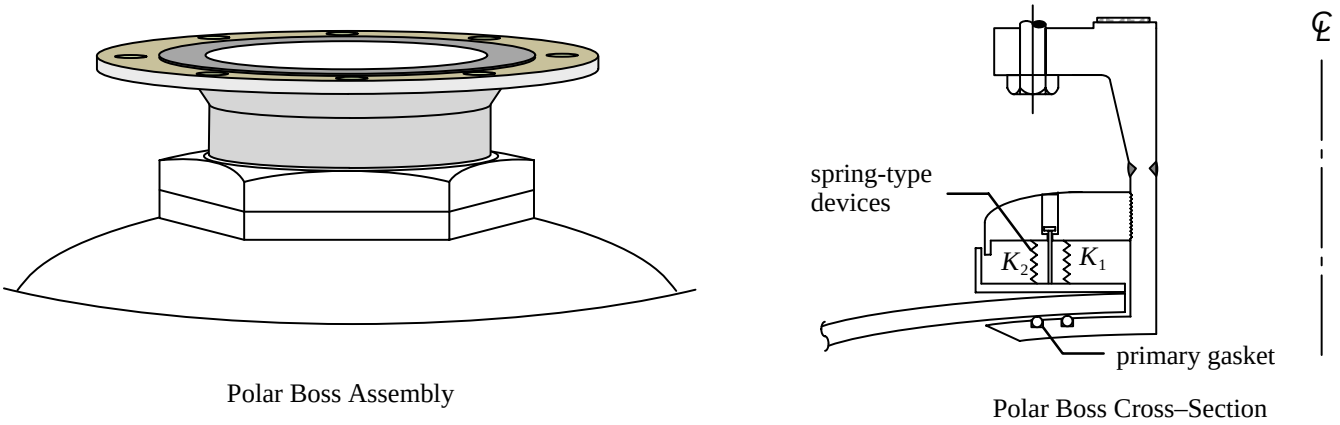

Figure 3: Polar Boss Assembly and Cross-Section.

Material permeability and leak testing of the composite dome test article and polar boss assembly is scheduled for mid-1999 in the CTF. The CTF is capable of testing tank domes with cryogenic liquids at pressures of up to 150 *psi* (1.03 *MPa* – megapascal). The major component of the CTF, the CTF assembly shown in Fig. 2, is supported on a five foot (1524 mm) high by ten foot (3048 mm) wide and ten foot (3048 mm) long I-beam frame that suspends the entire CTF assembly for easy access. The test article is sandwiched between two containment shells, creating two volumes. The pressurized fluid is contained in one volume, while the amount of fluid that diffuses through the test article wall over a period of time is measured in the other volume. A schematic of the cryostat test setup and facility piping is shown in Fig. 4. The test series for the composite dome test article consists of two parts. Phase I testing will verify the test setup at the CTF and provide baseline material permeability data for an intact test article. However, since pressure vessels include openings for access, the permeability characterization testing is also performed on a test article with a polar boss system installed. Therefore, after the testing on the intact test article is performed, an opening for the polar boss will be machined. Phase II will investigate the attachment and resulting permeability/leakage for the polar boss system. Therefore, the analysis and design are carried out for the intact dome first; then, the perforated dome is considered. In either case, an example of a typical test sequence for the entire test series is now given. A test sequence consists of five steps in pressure from fifteen *psi* (0.10 *MPa*) to seventy-five *psi*

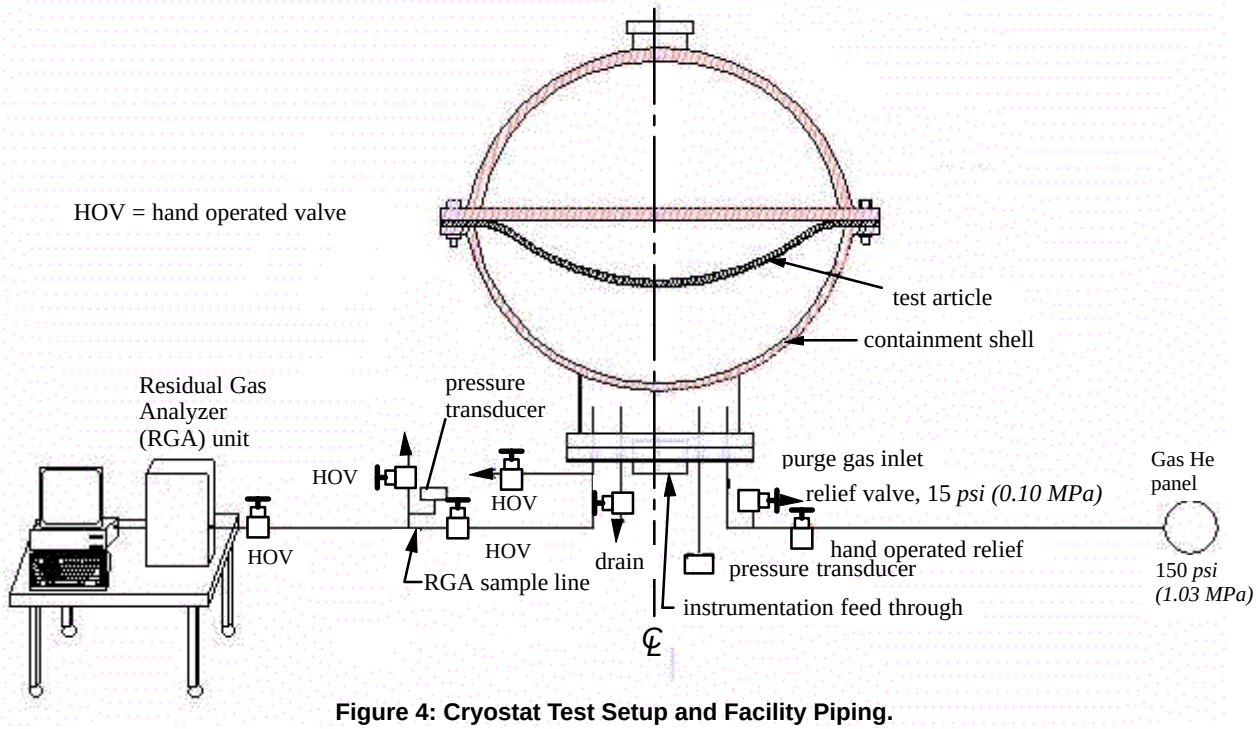

Figure 4: Cryostat Test Setup and Facility Piping.

(0.52 *MPa*), with the temperature being cycled by allowing the test article to warm to room temperature following each pressure step. First, a vacuum is pulled on the volume between the test article and lower containment shell to allow sampling of that volume with a residual gas analyzer. The residual gas analyzer monitors gases permeating or leaking through the test article. Then, the volume between the upper containment shell and the test article is filled with a liquid cryogenic fluid. Finally, the test article is pressurized to an amount between fifteen *psi* (0.10 *MPa*) and seventy-five *psi* (0.52 *MPa*) based on the current load step of the test sequence. The pressure is held at the given level until a steady-state measurement of the permeability is taken. Once the measurement is complete, the pressure is released and the tank drained to allow the tank to warm to ambient conditions in preparation for the next cycle.

DISCUSSION OF FAILURE MODES

We considered four possible failure modes in the design of the dome: (1) leakage at the joint of the cryostat assembly, Fig. 1; (2) the failure of the composite dome under internal pressure; (3) buckling of the dome during the line checkout condition; and (4) buckling of the dome during transportation. The first failure mode is addressed by the double o-ring gasket system, Fig. 1, Detail D, and is not covered in this study. The remaining failure modes are caused by three different loading conditions that will be addressed in this study. Since the test article is tested before and after the polar boss is installed, the remaining failure modes must be checked for the intact dome as well as after it has been perforated and the polar boss installed.

Intact Dome Case

For the intact dome, two possible loading conditions are considered, pressurization of the cryogenic fluid and a loading that may cause buckling of the dome. The loading condition associated with failure mode 2 is the maximum nominal internal pressure loading placed on the dome during the test sequence to determine material permeability, which is 75 *psi* (0.52 *MPa*). The loading condition associated with failure mode 3 occurs when the volume between the test article and the lower containment shell becomes pressurized, Fig. 4. The purpose of this pressurization is to test the cryostat facility lines for leaks. This loading condition is modeled with an external pressure of 15 *psi* (0.10 *MPa*), and we will refer to it as the “checkout condition”.

Perforated Dome with Polar Boss Case

The aforementioned two loading conditions for the intact dome also apply to this case. Also, the dome may experience a third loading condition during transportation, if the dome is carried on its flanged surface. This loading is due to the dead weight of the polar boss shown in Fig. 3; however, no pressure acts on the dome for this condition. Thus, each of these three loading conditions must be considered in the design of the perforated dome.

ANALYSIS AND DESIGN OF COMPOSITE DOME

The material properties used in the analysis were determined at a temperature of –65 °F (–54 °C), which is much higher than the cryogenic operating temperatures. However, elastic properties, such as strength and stiffness, generally increase as temperature decreases to cryogenic conditions (Barron, 1985). For this investigation, we use lamina elastic properties provided by the manufacturer for the dome design. These properties were used to obtain the effective isotropic properties listed in Table I. Lamination theory can be used to derive these effective isotropic properties (Agarwal and Broutman, 1990).

The only design variables needed to complete the design of the test article are the dome thickness and composite material lay-up. The thickness for the dome and the material lay-up are determined using the analysis procedures presented in the following sections (unlike isotropic designs, both variables are part of the design process). Even though there is an infinite number of lay-up combinations, we limit this design to a symmetric quasi-isotropic lay-up, (Agarwal and Broutman, 1990). This simplifies the analysis for the preliminary design. Since the intact dome is tested first and then perforated to install the polar boss system, the design of the perforated dome entails determining a secondary lamination system to reinforce the hole to attenuate the stress concentrations caused by the geometric discontinuity. That is, the design of the intact dome, thickness and lay-up, is used in the design of the perforated dome. In the next two sections we describe the details of the design for the dome and the reinforcement.

Intact Dome

For the preliminary design of the dome, we considered the failure of the dome under internal pressure, loading condition associated with failure mode 2. The analysis for this preliminary design of the dome was completed using membrane shell analysis. The stresses in the dome are uniform and are given by the following equation:

$$\sigma_\theta = \sigma_\phi = \frac{PR}{2h} = \sigma, \qquad (1)$$

where, P is the internal pressure, R is the dome radius, and h is

Table I: Effective Isotropic Properties for IM7/8552 $[0^\circ/90^\circ, \pm 45^\circ]_{3S}$ Lay-up.

Effective Modulus E, ksi (GPa)	Poisson’s Ratio, ν	Strength σ_u, ksi (MPa)
10,500 (68.9)	0.363	80 (551)

the dome thickness. The subscripts θ and ϕ represent the spherical coordinates of the dome. In this study, the maximum distortion energy theory or von Mises Theory is used to check for the onset of failure in the dome. Primarily, the maximum distortion energy failure criterion is used to predict failure in ductile materials. In our case, this theory was used mainly as a method for comparing the quasi-isotropic composite dome with other known isotropic candidate domes. Those comparisons are not documented in this report. According to the maximum distortion energy theory, failure by yielding occurs when the distortion strain energy per unit volume for combined stress is equal to the maximum elastic distortion energy per unit volume in simple tension (Ugural and Fenster, 1995). The von Mises stress, a stress equivalent quantity, can be utilized to predict the onset of failure. Therefore, the von Mises stress can be computed using the stresses given by Eq. (1), since these are equal to the principal stresses. To determine dome failure, the maximum von Mises stress is compared with the strength of the composite. During the preliminary design, we considered three different configurations or lay-ups, $[0°, \pm 30°]_{4S}$, $[0°, \pm 60°]_{4S}$, and $[0°/90°, \pm 45°]_{3S}$. The capacity provided by each lay-up was assessed by comparing its corresponding strength with the von Mises stress. The final design is based on a $[0°/90°, \pm 45°]_{3S}$ lay-up of Hercules IM7/8552 (carbon/epoxy) prepreg fabric, which has a strength of 80,000 *psi* (551 *MPa*), Table I. The results from this analysis are listed in the first column of Table II. This twelve ply lay-up results in a nominal dome thickness of 0.12 inches (3 mm). This is a quasi-isotropic lay-up which possesses isotropic in-plane stiffness properties, i.e., the extensional stiffness matrix, [A], is invariant with respect to in-plane rotations of the coordinate system. The bending properties, however, are still orthotropic. Nevertheless, the dome can be analyzed using the effective isotropic material properties without compromising practical accuracy. The material properties used in the analysis are given in Table I. These properties were derived from experimental data provided by Hercules, the material fabricator.

In addition to membrane stresses, the dome will experience flexural stresses and stress concentrations due to the geometry of the test article and configuration of the test setup. Thus, a finite element analysis was conducted using MSC/NASTRAN to determine the bending stresses, the stress around the geometric discontinuities, the overall deformations, and to assess the overall strength. The flange portion of the dome is partially unsupported, as shown on the cryostat assembly sketch in Fig. 1. This causes the radius of the flange-dome intersection to straighten upon loading, causing further stressing of the material. For this portion of the dome and other regions where stress concentrations cause excessive deformation and overstressing, instead of increasing the thickness of the entire dome, local reinforcement was designed to reduce these localized stresses. The finite element mesh for the dome model is depicted in Fig. 5 and consists of 437 CTRIA3 three node shell elements and 13,547 CQUAD4 four node shell elements (32 elements in the meridional direction and 437 elements in the circumferential direction). The loading for this case is the internal pressure loading associated with failure mode 2. The von Mises stress distribution in the dome is shown in Fig. 6. This figure clearly shows the stress concentration at the flange-dome intersection, and that this stress concentration is localized near the geometric discontinuity. This over-stressed part was reinforced with additional layers of carbon/epoxy cloth,

Table II: Results Summary for Intact Dome.

	No Flange Reinforcement			Reinforced Flange	
	Membrane analysis	Finite element analysis		Finite element analysis	
		No bending *	Maximum	No bending *	Maximum
$\sigma_\phi = \sigma_\theta$, *psi* (*MPa*)	*25,081 (172.9)*	*25,083 (172.9)*	–	–	–
$\epsilon_\phi = \epsilon_\theta$	*1.52E–03*	*1.52E–03*	–	–	–
w, *in* (*mm*)	*0.1221 (3.1)*	*0.1697 (4.3)*	*0.199 (5.0)*	*0.160 (4.1)*	*0.160 (4.1)*
von Mises, *psi* (*MPa*)	*25,081 (172.9)*	*25,027 (172.5)*	*64,500 (444.7)*	*25,000 (172.4)*	*43,400 (299.2)*
Buckling Analysis for Check-out Condition					
	Analytical			Finite element analysis	
	"Linear"		Non-linear		
λ_{cr}	*1.939*		*1.4*	*1.9605*	

* the region of the dome where no flexure occurs

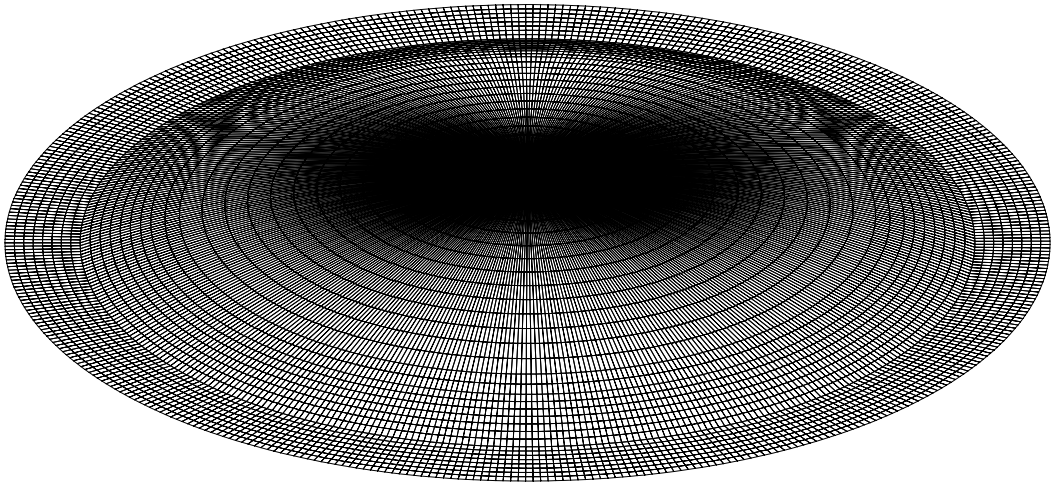

Figure 5: Dome Finite Element Mesh.

see Fig. 7. The lay-up for the reinforcement is similar to that for the dome, i.e., [0°/90°, ± 45°]. A summary of the results for the finite element analyses of the unreinforced and reinforced intact dome, is reported in Table II. This table shows that the membrane analysis results are in good agreement with the results of the finite element analysis for the portion of the dome where no bending occurs, the "no bending" results column in Table II. Although the 64.5 *ksi* (445 *MPa*) maximum stress for the unreinforced dome does not exceed the 80 *ksi* (551 *MPa*) strength allowable, we decided to reinforce the dome to attenuate the excessive deformation and stresses as well as to obtain a factor of safety against failure of approximately two. Therefore, the results for the reinforced dome in Table II provide a factor of safety of nearly two, based on the maximum von Mises stress for the reinforced flange of 43.4 *ksi* (299 *MPa*) and the 80 *ksi* (551 *MPa*) strength.

The other possible loading for the intact dome, the loading condition associated with failure mode 3, is the external pressure of 15 *psi* (0.10 *MPa*) applied during the CTF line checkout procedure. To assess the stability (buckling) of the dome under this loading, analytical and finite element analyses were conducted with the results listed on the bottom of Table II. These results are presented in terms of critical eigenvalues. The critical external pressure can be determined by multiplying the critical eigenvalue by the external pressure, i.e., $\lambda_{cr} = P_{cr}/P_{appl}$. The "linear" analytical solution was obtained using the following equation (Harvey, 1991):

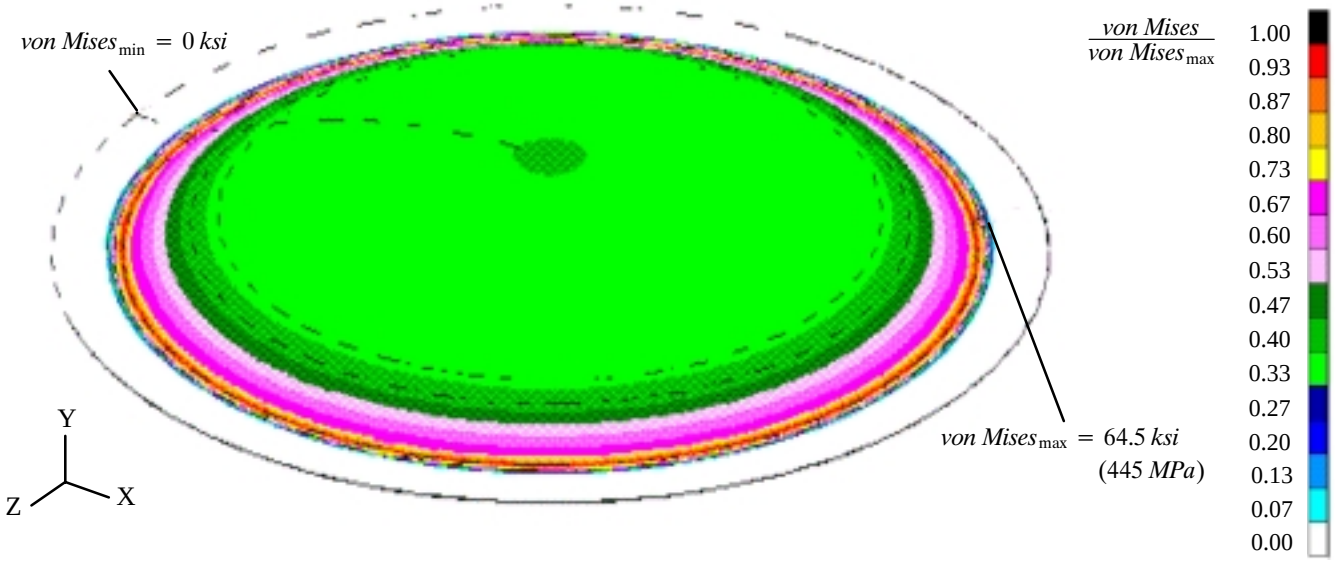

Figure 6: von Mises Stress for Intact Dome.

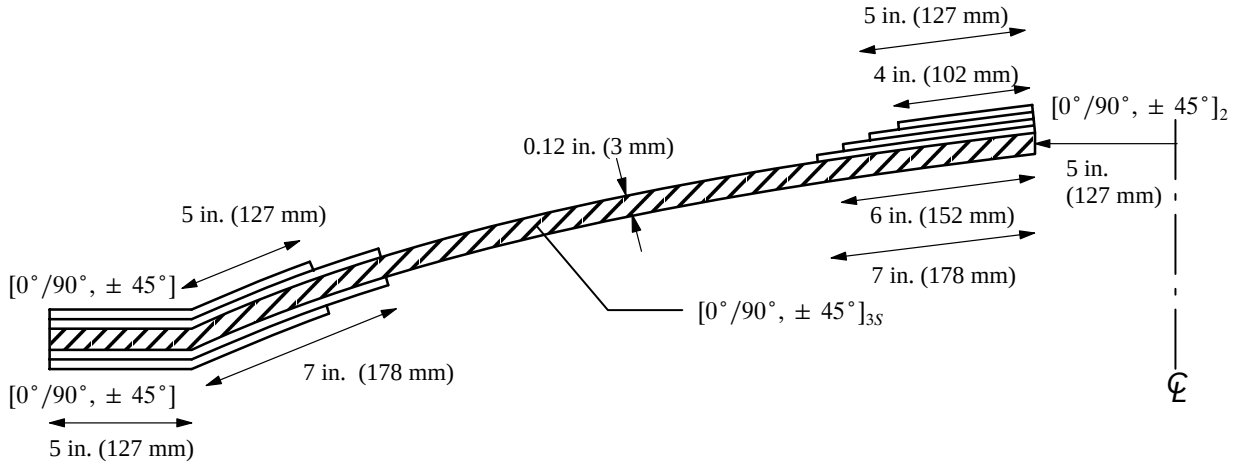

Figure 7: Dome and Reinforcement Lay-up.

$$\lambda_{cr} = \frac{2E}{P[3(1-\nu^2)]^{1/2}}\left(\frac{h}{R}\right)^2, \qquad (2)$$

where, E is Young's modulus and ν is Poisson's ratio, the other quantities were defined after Eq. (1). This solution does not account for prebuckling nonlinearity or deformation; therefore, we categorize the analysis as "linear". Although Eq. (2) was derived for a clamped shallow spherical shell, the results seem to be in good agreement with those obtained from the linear static buckling finite element analysis. The prebuckling nonlinearity or deformation was not taken into account in the finite element analysis either. The nonlinear buckling analytical solution was obtained from Fig. 37 in Bushnell (1989). This figure in Bushnell depicts a plot for the stability of a shallow spherical dome generated using nonlinear numerical analysis and experimental test data. Based on a cap shallowness parameter, $2[3(1-\nu^2]^{1/4}(H/h)^{1/2}$, of approximately 17 for our composite dome test article, the critical pressure for the nonlinear case is determined using the test data on the plot, i.e. $P_{cr}/1.2E(h/R)^2 = 0.74$. Therefore, using the experimental results to determine the critical eigenvalue for the nonlinear case, the shell is considered safe against buckling during the line checkout condition, i.e., $P_{cr}/P_{appl} \backsim 1.4$.

Perforated Dome with Polar Boss

In order to access the interior of a pressure vessel, an opening is required. Therefore, a circular opening will be machined at the polar region of the intact dome described in the last section. A boss or a stub flange is used to connect the pressure vessel to the line that carries the fluid to and from the pressure vessel. In composite pressure vessels, this boss is typically metallic, see Fig. 3. The geometric discontinuity that the hole presents causes a stress concentration near the opening. As shown in Fig. 6, the stress state in the polar region of the intact dome is uniform, and the two principal stresses are equal. Based on this observation, the variation of stress in the region of the circular hole can be computed using the following equation (Harvey, 1991):

$$\sigma_c = \sigma\left(1 + \frac{a^2}{r^2}\right) \qquad (3)$$

where, σ is the membrane stress, a is the radius of the circular polar opening, and r is the meridional distance from the center of the hole. Notice that the stress decreases rapidly as the distance from the edge of the hole increases. At the edge of the hole, $r = a$ and the maximum stress is 2σ, Eq. (3). At a distance from the edge of the hole equal to the radius, $r = 2a$, the stress has fallen to 1.25σ. The von Mises stress at the edge of the hole can easily be determined since one principal stress is zero and the other is given by Eq. (3); the results are listed in Table III. The reinforcement around the circular hole is designed to reduce this stress concentration. The reinforcement lay-up is depicted in Fig. 7. This lay-up eliminates the symmetry of the overall lay-up; however, the bending-extension coupling effect should be small since the polar boss clamps this region.

We again conducted finite element analyses of the dome using MSC/NASTRAN, with and without the reinforcement around the circular opening. The mesh for this analysis consisted of 6,976 CQUAD4 four node shell elements (32 elements in the meridional direction and 218 elements in the circumferential direction). The results are listed in Table III. Figure 8 shows the distribution of the von Mises stress. In this part of the design, we also had to take the weight of the polar boss into account. The weight of the polar boss was estimated at 40 pounds (18.14 Kg) from a previous design. This weight was applied as a ring load, equivalent to 1.28 pounds per inch (0.22 N/mm) at the edge of the hole. Also, the boundary conditions at the edge of the hole are not well defined. We considered two cases, shown in Fig. 9. In the first case, the polar boss provides complete clamping of the edge of the hole, allowing only vertical displacements of the edge. For the second case, the edge of the hole is allowed to slide

Table III: Results Summary for Dome with Circular Opening.

No Circular Opening Reinforcement					
	Analytical (Harvey)	Finite–Element Analysis			
		Clamped hole edge		Semi–Free hole edge	
		No Bending*	Maximum	No Bending*	Maximum
w, in. (mm)	–	*0.150 (3.8)*	*0.151 (3.8)*	*0.150 (3.8)*	*0.467 (11.9)*
von Mises, psi (MPa)	*50,162 (345.9)*	*27,000 (186.2)*	*43,400 (299.2)*	*27,000 (186.2)*	*98,400 (678.4)*
Reinforced Circular Opening (finite–element analysis)					
	Clamped hole edge		Semi–Free hole edge		
	No bending*	Maximum	No bending*	Maximum	
w, in (mm)	*0.160 (4.1)*	*0.160 (4.1)*	*0.160 (4.1)*	*0.270 (6.9)*	
von Mises, psi (MPa)	*27,000 (186.2)*	*43,200 (297.9)*	*27,000 (186.2)*	*62,400 (430.2)*	
Buckling Analysis for Check-out Condition (finite–element analysis)					
P_{cr}	*29.27 psi (0.202 MPa)*				

* the region of the dome where no flexure occurs

freely between the clamping system of the polar boss, restraining only rotations but not displacements. We believe the true condition is somewhere in between, but closer to the clamped hole condition. However, from Table III, we can see that even the most conservative case results in a maximum possible stress for the reinforced hole of 62.4 *ksi* (430 *MPa*) which does not exceed the strength of the composite, 80 *ksi* (551 *MPa*).

The line checkout condition for this part of the investigation is also safe against buckling, as shown at the bottom of Table III, $\lambda_{cr} = P_{cr}/P_{appl} = 1.9514$. This result was obtained using finite element analysis for the perforated dome with the clamped boundary condition, loaded with the external pressure of 15 *psi* (0.10 *MPa*) applied during the CTF line checkout procedure.

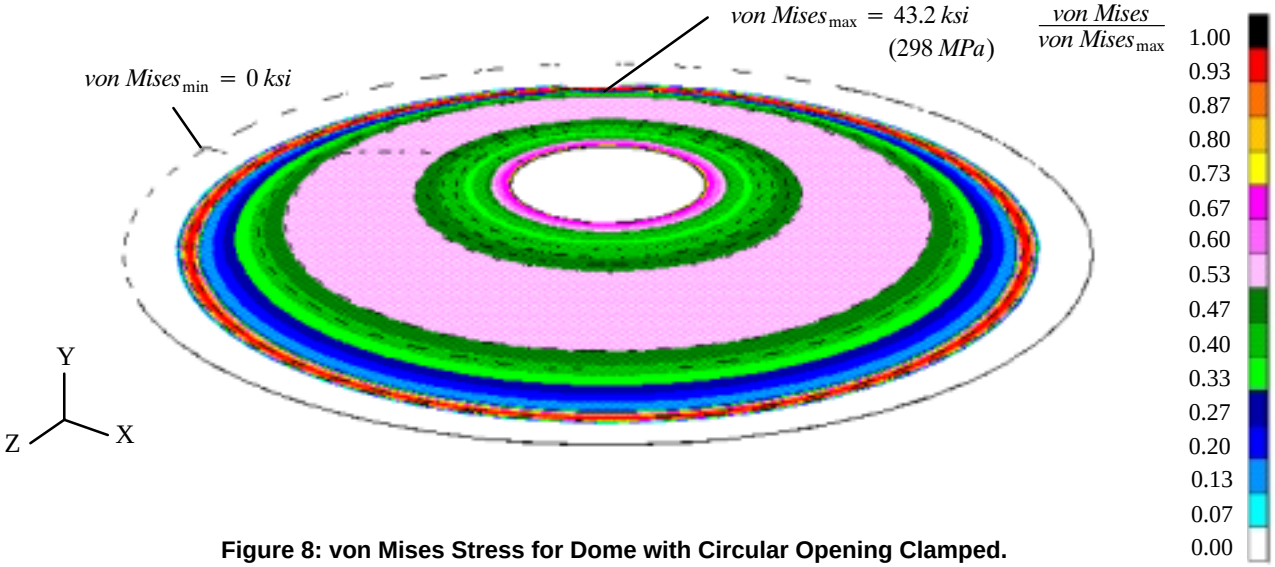

Figure 8: von Mises Stress for Dome with Circular Opening Clamped.

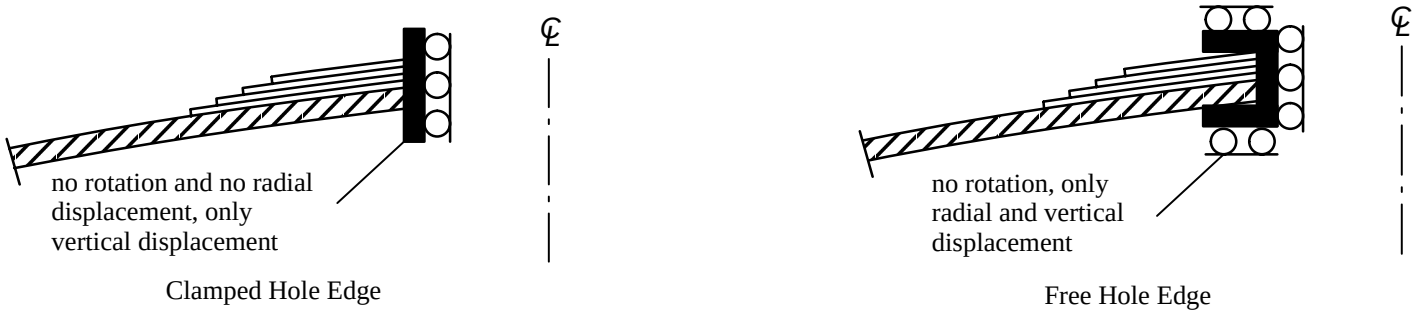

Figure 9: Boundary Conditions for Finite Element Analysis of Perforated Dome.

For this part of the investigation, we also had to consider an additional loading condition, the weight of the polar boss when the dome is transported upside down. The weight of the polar boss is 40 pounds (18.14 *Kg*), which is equivalent to a 1.28 pounds per inch (0.22 N/mm) ring load on the edge of the hole. The resulting stresses determined using finite element analysis are negligible. Therefore, this loading is negligible and does not cause any detrimental instability or stress concentrations.

DESCRIPTION OF POLAR BOSS SYSTEM

Access systems are required in all pressure vessels; a polar boss system is employed in the test article presented in this paper. A requirement of all access systems is to contain the fluid with minimum leakage, since all access systems leak at some level. To minimize leakage, this type of polar boss system is often sealed with two o-ring gaskets, i.e., a second gasket is placed adjacent to the primary sealing gasket, see Fig. 3. It is difficult for a flat rigid polar boss assembly to conform to the curvature of the dome. In our case, a flat rigid polar boss assembly does not compress the two sealing gaskets uniformly or with adequate pressure. To obtain the same compression on both gaskets, additional force must be applied on the part of the dome near the primary gasket because this gasket is located further from the center line of the boss assembly. To solve this problem, we developed an innovative design for the polar boss, Fig. 3. The improved polar boss design has a flexible washer that conforms to the curvature of the dome, applying uniform compression to both gaskets. The design consists of two interlocking rings that sandwich two spring-type components. These spring-type components are placed at the same distance from the center line of the boss assembly as the o-ring gaskets. A unique feature is that each of the spring-type devices may have a different stiffness, which allows each spring-type device to transfer a different amount of force. The different spring stiffnesses can be chosen such that their resulting forces compress the two o-ring gaskets with the same amount of force, thus making the sealing system more effective.

CONCLUDING REMARKS

In this paper, a method is presented for designing composite pressure vessels with a combination of membrane and finite element analyses. The membrane analysis can be used as a preliminary design tool; then, parts of the system where bending and stress concentrations are possible can be investigated using a finite element analysis. We made use of this analysis tool combination in the design of a CFRP dome cap and flange for material permeability characterization. In regions where stress concentrations or gradients occur, rather than increasing the thickness of the entire dome, additional layers of carbon/epoxy cloth are used to attenuate these stress concentrations. Thus, a complete numerical investigation of the critical load cases for the CFRP dome test article have provided analytical results which show the test article remains below required stress levels.

ACKNOWLEDGEMENTS

The authors would like to thank the NASA/MSFC Center Director's Discretionary Fund office and the NASA/ASEE Summer Faculty Fellowship program for making this research possible. We would like to thank Bill McMahon, Seth Lawson, and personnel of EH35/MSFC and the Thiokol Corporation for the fabrication of the test article. Thanks to Kathryn Horton and Scott Lauffer of ED51/MSFC for providing essential engineering drawing support and Russ Abrams and Mat Bevill of EP91/MSFC for test configuration drawings.

REFERENCES

Agarwal, B. D. and Broutman, L. J., 1990, "Analysis and Performance of Fiber Composites," 2nd edition, John Wiley & Sons, Inc., New York.

Barron, R. F., 1985, "Cryogenic Systems," Oxford University Press, New York.

Bushnell, D., 1989, "Computerized Buckling Analysis of Shells," Kluwer Academic Publisher, Boston.

Harvey, J. F., 1991, "Theory and Design of Pressure Vessels," Chapman & Hall, New York.

Ugural, A.C. and Fenster, S.K., 1995, "Advanced Strength and Applied Elasticity", 3rd edition Prentice Hall, Upper Saddle River, New Jersey.